Controlling Chain Growth: A New Strategy to Hyperbranched Materials

Wenxin Wang,*,† Yu Zheng,† Emma Roberts,† Christopher J. Duxbury,† Lifeng Ding,† Derek J. Irvine,‡,§ and Steven M. Howdle*,†

School of Chemistry, University of Nottingham, Nottingham, NG7 2RD, England, and School of Chemical, Environmental and Mining Engineering, University of Nottingham, Nottingham, NG7 2RD, England

Received March 23, 2007; Revised Manuscript Received July 3, 2007

ABSTRACT: Hyperbranched polymers with both highly branched structures and numerous vinyl functional groups have been synthesized via reversible activation/deactivation controlled polymerization of multifunctional vinyl monomers. By controlling the competition between propagation and reversible termination using a deactivation enhanced method, the growth rate of polymer chains is decreased and the onset of gelation is prevented until the system has achieved much higher levels of conversion than has previously been reported for nonenhanced systems. Here, we demonstrate this strategy by synthesizing highly branched, irregular dendritic polymers with a multiplicity of reactive functionalities such as vinyl and halogen functional groups, and controlled chain structure via deactivation enhanced atom transfer radical polymerization (ATRP) of a commercially available multifunctional vinyl monomer—divinylbenzene (DVB) and ethylene glycol dimethacrylate (EGDMA).

Introduction

Dendritic materials have captured the imagination in a variety of multidisciplinary areas.[1−5] The three-dimensional structure of these materials has made them attractive for applications ranging from drug delivery[6] to nanobuilding blocks.[7−9] However, regular dendrimers are only accessible through complicated multistep syntheses, which limits their availability. By contrast, hyperbranched polymers with less well-defined structure may be synthesized more easily,[10−13] but effective synthesis has been restricted to a few AB_n monomers and inimers.[14−16] The combination of these factors has severely impaired the commodity application of dendritic materials.

In free-radical polymerizations, the inclusion of only small amounts of multifunctional vinyl monomer leads to production of a cross-linked network. Sherrington[17] and Guan[18] reported chain transfer controlled conventional free radical polymerization routes to branched polymers using multifunctional vinyl monomers as the branching species. Gelation was inhibited by use of thiol or catalytic chain transfer (CCT) species. Sato reported a chain termination controlled free radical polymerization route—initiator-fragment incorporation radical polymerization (IFIRP).[19] However, these methods cannot provide control of the molecular weight and branched structure of the polymers because of their non living nature. Living radical polymerizations have more recently been investigated because chain transfer and termination can be suppressed by the low radical concentration. Sherrington and Armes[20] improved the methodology significantly by introducing controlled or living polymerization and by controlling the level of the branching multifunctional vinyl monomer employed. The copolymerization of methyl methacrylate (MMA) and ethylene glycol dimethacrylate (EGDMA) using Cu-based ATRP and group transfer (GTP) polymerizations were reported, and low concentrations of multifunctional vinyl monomer were found to be essential. In addition, the mole ratio of this branching monomer to initiator was limited to less than 1 to form soluble branched polymer, and avoid cross-linking. When this ratio exceeds 1, only an insoluble cross-linked network or microgel was produced. Perrier[21] adopted a similar procedure using reversible addition fragmentation chain transfer (RAFT). The end result in all cases is that the copolymers produced are predominantly formed from monofunctional vinyl monomer and have only a low degree of branching.

Developing new synthetic routes to such polymeric materials is of great interest and a method that can directly polymerize existing commodity monomers to form dendritic materials with controlled architecture will be highly desirable. We now report a facile and versatile approach to the formation of highly branched polymer architectures through a reversible activation (or deactivation) controlled polymerization of multifunctional vinyl monomer. Our strategy overcomes the published limitations, and most importantly, there is no restriction on the concentration of multifunctional vinyl monomer. Indeed, we demonstrate that multifunctional vinyl monomers can even be homopolymerized to form hyperbranched polymer structures rather than cross-linked networks. The key has been to find a method for slow growth of each independent and complex hyperbranched molecule that avoids cross-linking. We realized that by controlling the competition between chain growth and reversible chain termination via a deactivation enhanced method, polymers can grow effectively, branching is introduced by multifunctional vinyl monomer in a controlled fashion and cross-linking is prevented, which leads to the formation of hyperbranched polymers. Scheme 1 outlines the basic concept: a multifunctional vinyl monomer (A) is selected with a catalyst system (I* + X) where I* is capable of initiating the polymerization of vinyl monomer (e.g., by means of radical, cationic, group transfer, or ligated anionic polymerization) to produce a

* To whom correspondence should be addressed: E-mail: (W.W.) wenxin.wang@nottingham.ac.uk; (S.M.H.) steve.howdle@nottingham.ac.uk. Telephone: 0115 951 3486. Fax: 0115 951 3058.

† School of Chemistry, University of Nottingham.

‡ School of Chemical, Environmental and Mining Engineering, University of Nottingham.

§ Former address: Uniqema, Wilton Centre, Wilton, Redcar, TS10 4RF, England.

10.1021/ma0707133 CCC: $37.00
Published on Web 09/05/2007

Scheme 1. Strategy for Reversible Activation (or Deactivation) Controlled Hyperbranch Polymerization Process

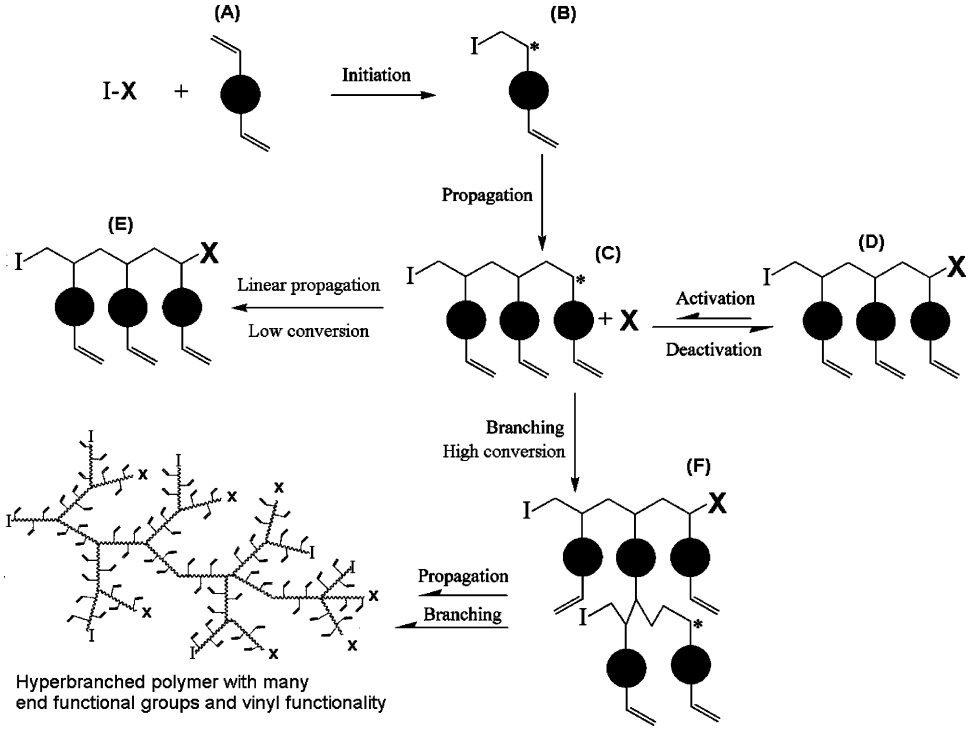

multivinyl macromonomer chain (C). Catalyst (X) can establish an equilibrium between the active macromonomer chain (C) and dormant macromonomer chain (D). The dormant species (D) can be converted to the active species (C) by thermal, photochemical, and/or chemical stimuli. In this way, all of the growing macromolecules are subject to a rapid equilibrium between active and dormant states: a reversible activation (deactivation) equilibrium. Unlike normal propagation whereby monomers are sequentially added into a polymer chain, here the active species (C) can undergo two different mechanisms of propagation: either linear chain growth by simple addition of monomer (A) to the existing chain, or formation of branched polymer chains by addition of multi vinyl macromonomer into the growing chain (F). What is crucial is that, in both cases, the equilibrium between the active and dormant species allows slow, controlled growth of the polymer chains. Thus, cross-linking reactions are suppressed efficiently. At low monomer conversion, statistics dictate the formation of predominantly linear polymer chains with moderate branching. However, at higher monomer conversion, highly branched structures are formed due to the increased participation of multivinyl macromonomers in the reaction. Hence, at high monomer conversion the reaction is driven toward the formation of highly branched species (Scheme 1, structure F). The key is to allow the growth of each independent and complex hyperbranched molecule, but to avoid rapid cross-linking between the molecules. This can be achieved by manipulating the equilibrium to increase the deactivation rate and decrease the activation rate and thus slow down the growth rate of polymer chains, e.g., for ATRP, the addition of Cu(II) species to the system slows down propagation. In this paper, we demonstrate this strategy by synthesizing highly branched poly(DVB) and poly(EGDMA) with a multiplicity of reactive functionalities such as vinyl and halogen functional groups, and controlled chain structure via deactivation enhanced ATRP, with the only key restriction on the process to prevent the manufacture of insoluble gels is that the overall conversion of monomer to polymer is limited to less than 60% of the total monomer feed.

Experimental Section

Materials. DVB and EGDMA monomer (Aldrich) was purified by passing through a column of activated basic alumina (ACROS) and purging with high-purity nitrogen for 1 h prior to use. Initiator stock solution was prepared from methyl 2-bromopropionate or methyl 2-chloropropionate (Aldrich) with 2-butanone (99.5+%, HPLC grade, Aldrich). The concentration of the methyl 2-bromopropionate or methyl 2-chloropropionate was 0.815 mol L^{-1}, and was degassed by high-purity nitrogen. 2,2′-bipyridine (bpy, Aldrich), copper(I) bromide (98%, Aldrich), copper(II) bromide (98%, Aldrich), copper(I) chloride (98%, Aldrich), and copper(II) chloride (99%, Lancaster) were used as received. Nitrogen was bubbled through the solutions in order to eliminate molecular oxygen. Liquids were transferred under nitrogen by means of septa and syringes or stainless steel capillaries.

Polymerization Procedure. Homopolymerization of Poly(DVB). Known amounts of CuBr, $CuBr_2$, and bpy were added to a round-bottom flask fitted with a three-way stopcock connected to either a nitrogen line or a vacuum pump. Oxygen was removed by repeated vacuum−nitrogen cycles. Once filled with nitrogen, the flask was filled with known amounts of degassed DVB and toluene. After the reaction was stirred for 1 h at room temperature, a known amount of methyl 2-bromopropionate was added, and the polymerization was conducted at the desired temperature. After polymerization under stirring at the chosen reaction temperature (typically 90 °C) for the desired reaction time, the solution was diluted with THF and precipitated into a large excess of methanol. After separation by filtration, the polymer was dried under reduced pressure at 30 °C and weighed in order to calculate the monomer conversion.

Homopolymerization of Poly(EGDMA). Known amounts of $CuCl/CuCl_2$ and bpy were added to a round-bottom flask fitted with a three-way stopcock, which was connected to either a nitrogen line or a vacuum pump. Oxygen was removed by repeated vacuum-nitrogen cycles. Once filled with nitrogen, the flask was charged with known amounts of degassed EGDMA and THF, and stirred at room temperature for 1 h. Then, a known amount of methyl 2-chloropropionate was added, and the polymerization was conducted at the desired temperature under stirring. After the desired polymerization reaction time, the solution was diluted with THF and precipitated into a large excess of hexane. After separation by

Scheme 2. General ATRP Reaction Mechanism

$$P_n\text{-Cl} + Cu^{I}Cl/L \underset{k_{da}}{\overset{k_a}{\rightleftharpoons}} P_n^{*} + Cu^{II}Cl_2/L$$

Table 1. Homopolymerizations of DVB by Deactivation-Enhanced ATRP[a]

			GPC RI results		
reaction	DVB:[I]:Cu(I):Cu(II) feed ratio (mol)	time	M_n (g mol^{-1})	M_w/M_n	yield (%)
1	57: 1: 0.5: 0	5 h	14 000	8.5	20.7
2	57: 1: 0.5: 0.167	17 h	10 500	4.9	49.5
3	57: 1: 0.4: 0	6 h	14 200	22.7	21.5
4	57: 1: 0.4: 0.133	28 h	13 600	20.2	61.6
5	57: 1: 0.4: 0.2	32 h	6700	3.2	27.1
6	57: 1: 0.25: 0.25	36 h	3900	1.7	16.6
7[a]	57:1:0:0	5 min			gel

[a] Reaction 7 is a normal radical solution polymerization using azobis(isobutyronitrile) (AIBN) as initiator. A high ratio of Cu(II)/ Cu(I) significantly slows the reaction rate leading to high yields of hyperbranched polymer without formation of gels. Reaction conditions: [DVB] = 3.51 M, [Cu(I) + Cu(II)]/[bpy] = 1:2; all polymerizations were conducted under nitrogen in toluene at 90 °C.

filtration, the polymer was dried under reduced pressure at 30 °C and weighed to calculate the yield.

Characterization of Hyperbranched Polymers. Gel Permeation Chromatography (GPC) Characterization. Number-average molecular weight (M_n), weight-average molecular weight (M_w) and polydispersity (M_w/M_n) were obtained by gel permeation chromatography (PL-120, Polymer Labs) with an RI detector. The columns (30 cm PLgel Mixed-C, 2 in series) were eluted by THF and calibrated with polystyrene standards. All calibration and analysis were performed at 40 °C and a flow rate of 1 mL/min. All of the products easily dissolve in THF, and pass through 0.2 μm filter before injection with little or no backpressure observed—demonstrating the absence of gelation.

Multiangle Light Scattering−Size Exclusion Chromatography (MALLS/SEC). The instrument package was supplied by Wyatt and comprised the following equipment: (i) a Jones Chromatography 760 series Solvent D-Gasser, (ii) a Waters 515 HPLC pump operating at room temperature, (iii) a Jasco AS-950 autosampler with 50 position sample racks, (iv) a column oven, (v) a set of 30 cm PLgel Mixed-C, 2 in series, and (vi) a detector connected in a serial configuration—a multiangle light scattering detector (mini-Dawn) supplied by Wyatt Technology. The Astra software package for Windows was used to process the data from the detector systems to produce the weight-average molar mass, radius of gyration and molar mass vs elution volume plots.

NMR Analysis of the Polymers. ^{1}H NMR was carried out on a 300 MHz Bruker NMR with MestRec processing software. The chemical shifts were referenced to the lock $CDCl_3$.

Dynamic Light Scattering (DLS). The size distribution of linear polystyrene and hyperbranched poly(DVB) were measured by employing dynamic light scattering via Zetasizer nano series (Malvern instruments Ltd). The polystyrene standard sample is used as received, the molecular weight is 5000, 9800, 21000, 39000, 72200, 151700, 325000 respectively and PDI is less than 1.1. (Polymer Laboratories). The scattering angle was fixed at 90°. And the measurements were recorded at a constant temperature 20 °C. Each sample was filtrated through a 0.2 μm filter directly into a precleaned quartz curvet. The sample concentration was maintained at 1 mg/mL in the case of M_w less than 50 000 and maintained at 0.5 mg/mL in the case of M_w greater than 50 000.

Results and Discussion

Synthesis and Characterization of Hyperbranched Poly(DVB). The rate of polymerization of divinyl monomer by ATRP is first order with respect to concentration of monomer, initiator, and Cu(I) complex, and inversely proportional to Cu(II) concentration (Scheme 2).[22,23] Thus, control over the polymerization rate can be obtained by manipulating the feed ratio of Cu(I)/Cu(II) (eq 1). An increase in the concentration of Cu(II) relative to Cu(I) pushes the equilibrium toward the deactivated state. As the ratio of propagation to deactivation decreases, fewer monomer units are added to an active center before being deactivated, resulting in slow growth of polymer chains. We have found that this deactivation enhanced ATRP leads to preparation of soluble hyperbranched polymers rather than cross-linked gels provided the overall conversion of monomer to polymer is limited to less than 60%.

Equation 1 shows the kinetic equation of ATRP. k_p is the propagation rate constant, [M] is the concentration of the monomer, [R] is the concentration of radicals, K is the equilibrium constant, [R−X] is the concentration of halide initiator, and [Cu(I)] and [Cu(II)] are the concentrations of copper(I) and copper(II), respectively.

$$R = k_p[M][R] = k_pK[M][R-X]\frac{[Cu(I)]}{[Cu(II)]} \qquad (1)$$

For homopolymerization of DVB in toluene, the absence of Cu(II) species (entries 1 and 3, Table 1) leads to two observable effects on the polymerization. The first is that under certain conditions more rapid polymerization was achieved due to the reduced deactivation levels being applied and second, in all cases, the systems quickly lead to insoluble gels. In the typical experimental run under standard ATRP conditions, the polymerization progressed in the early stages in a similar manner to those of the equivalent deactivation enhanced examples. Thus, at low conversions in these conventional ATRP reactions the synthesis of hyperbranched species is observed in these systems. The GPC data reported in Table 1 refer to these hyperbranched species isolated at these low yield points in the experiments (entries 1 and 3). However as the synthesis progresses, it is noted that at yields above 20−25% the systems completely gel, making further reaction and analysis by GPC impossible. The highest yield of soluble polymer that can be achieved under these conditions was only ca. 20%. Adding Cu(II) enhances the rate of deactivation; the polymerization rate is significantly decreased and high yields of soluble hyperbranched polymer are obtained with controlled molecular weight (entries 2, 4, and

Table 2. Detailed Data of Hyperbranched DVB Samples of Reaction 4 Collected at Different Times, for Reaction Conditions [DVB] = 3.51 M and [Cu(I) + Cu(II)]/[bpy] = 1:2, in Toluene at 90 °C

			GPC results			MALLS results			
sample	reaction time (h)	yield (%)	M_n (g mol^{-1})	M_w (g mol^{-1})	M_w/M_n	M_n (g mol^{-1})	M_w (g mol^{-1})	M_w/M_n	branch ratio[a]
4−1	4	2.7	3000	3820	1.26	4496	5805	1.29	0.15
4−2	6	12.8	4450	7130	1.6	6867	12 830	1.87	0.21
4−3	10	28.8	7800	30 000	3.85	23 040	126 950	5.51	0.25
4−4	18	36.3	11 400	96 100	8.39	103 600	625 400	6.04	0.28
4−5	28	61.6	13 600	275 900	20.2	885 900	5 373 000	6.07	0.33
4−6	30	65	gelation						

[a] Branch ratio from NMR data (see Figure 2 and eq 2)

5). Kinetic plots (Figure S1 in Supporting Information) show the evolution of the ATRP controlled reactions of these reactions, and most significantly, demonstrate that the yields can be pushed to high levels, e.g., 61.6% (entry 4). Addition of too much Cu(II) with respect to Cu(I) over suppresses the polymerization (entries 5 and 6) giving only low conversion. Despite the very long reaction times, no cross-linking is observed, a point which is further emphasized by comparison of entries 3 and 4. Clearly, cross-linking and gel formation does eventually occur in these systems, but only when the conversion is pushed beyond 65% (Table 2)

The molecular weight evolution of entry 4 was studied in more detail by collecting samples throughout the reaction (Table 2 and Figure 1). GPC traces (Figure 1) obtained by refractive index (RI) and multiangle light scattering (MALLS) detectors clearly show increase in molecular weight and broadening of polydispersity with reaction time. These data provide sound evidence for formation of hyperbranched poly(DVB). Initially, statistics dictate the formation of predominantly linear polymer chains with moderate branching, and the molecular weight distribution is narrow at low monomer conversion ($M_{w,RI}/M_{n,RI} = 1.26$ and $M_{w,MALLS}/M_{n,MALLS} = 1.3$ at 4 h). As the reaction progresses, both molecular weight and polydispersity increase dramatically because of the increased participation of multivinyl macromonomers at high monomer conversion ($M_{w,RI}/M_{n,RI} = 20.2$ and $M_{w,MALLS}/M_{n,MALLS} = 6.0$ at 28 h). This also indicates why the conversion restriction is important in this synthetic method. At below 60%, the balance of monomer to macromer is such that significant macromer:macromer reaction is prevented in favor of macromer:monomer by virtue of molar fraction, steric bulk and molecular mobility effects. However, above this conversion threshold, the barriers to intermacromer reaction are significantly reduced, thus allowing gel formation to occur.

The data show that the measured MALLS molecular weight is always higher than the RI results, strongly supporting formation of a hyperbranched architecture.[24] Further, the GPC and MALLS data for sample number 5 (Tables 1 and 2 and Figure 1) demonstrate a significant issue encountered in the analysis of the materials produced in this program of work. It is clear from comparison of the GPC and MALLS data that there is a significant difference in the measured M_w and PDIs for the same sample from these differing detector systems. This is very likely to be due to the highly branched nature of the structures being produced. It is believed that the MALLS data is the more trustworthy and representative of the true M_w of these systems and that the RI system is underestimating the true molecular weights very significantly as a result of the 3-dimensional shape of the polymers synthesized. Furthermore, our use of GPC equipment which has operational limits from 2000 to 2 million Da (M_w), has a clear effect upon the data obtained. It is clear from the MALLS data that the material isolated in sample 5 has a significant component above the upper exclusion limit of the system and thus cannot give definitive molecular weight nor polydisperstiy data for this particular sample. It has been included for comparison with the materials sampled at earlier points in the reaction only to demonstrate that the molecular weight of the hyperbranched material is certainly still rising at this point but has not yet become an insoluble gel.

^{1}H NMR analysis also confirms the formation of a hyperbranched structure for poly(DVB). The presence of a multiplicity of reactive and potentially useful vinyl functionalities is clearly demonstrated (peaks c and d from the vinyl functional group and peaks g and h from the end functional group in Figure 2). Moreover, comparison of the integrals of the backbone and vinyl

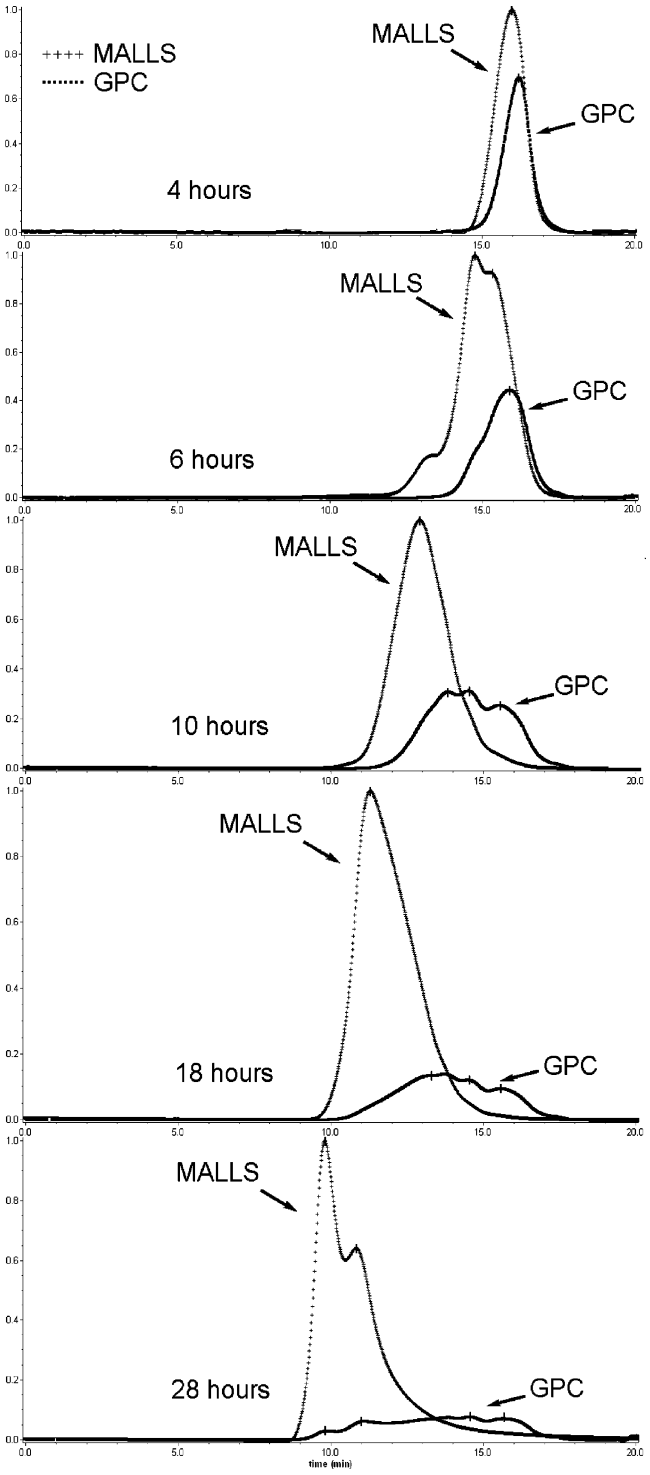

Figure 1. MALLS and RI chromatograms for the GPC analysis of poly(DVB) isolated at different reaction times (entry 4, Table 1 and Table 2). The molecular weight and polydispersity clearly show the increase with reaction time, which support the formation of hyperbranched polymer with controlled chain structure.

protons allows an approximation of the ratio of branched to linear DVB (eq 2). From the NMR analysis, our novel method produces a much higher branched ratio (from 15% to 33%) than previous published methods have reported (from 5% to 15%).[25] The equation used to calculate this branching number is shown as eq 2. For reaction 4 (Table 1) NMR data can be used to follow the steady increase of the degree of branching as monomer conversion increases (Table 2), the final product achieving a ratio of 0.33. The molar fraction of branched DVB

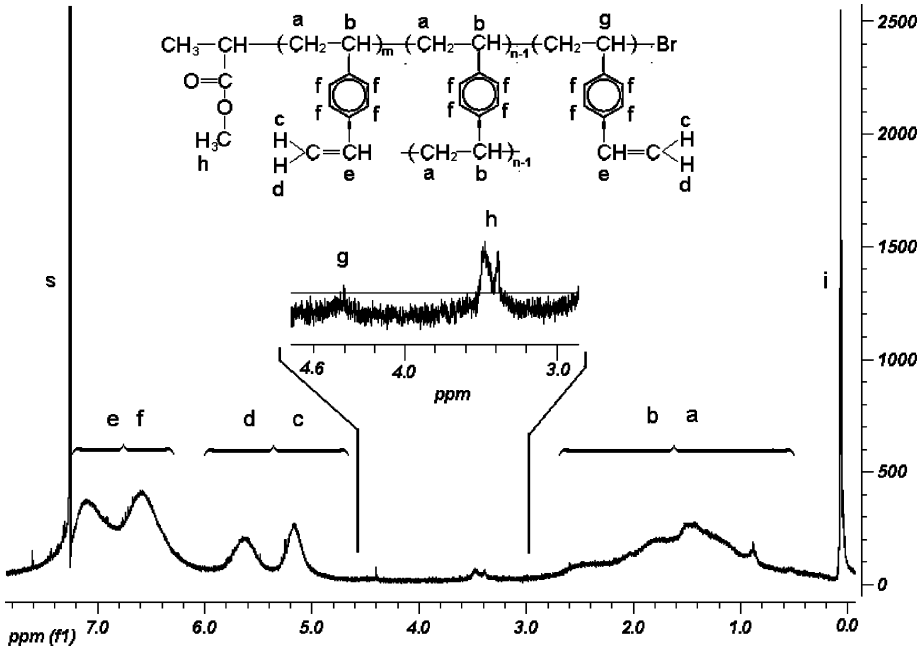

Figure 2. [1]H NMR spectrum of hyperbranched poly(DVB) (entry 4; Table 1). Comparison of backbone (a, b) and vinyl (c, d) enables determination of branching ratio (Table 2). Peaks c, d, g, and h show clear presence of vinyl functionalities and terminal functional groups.

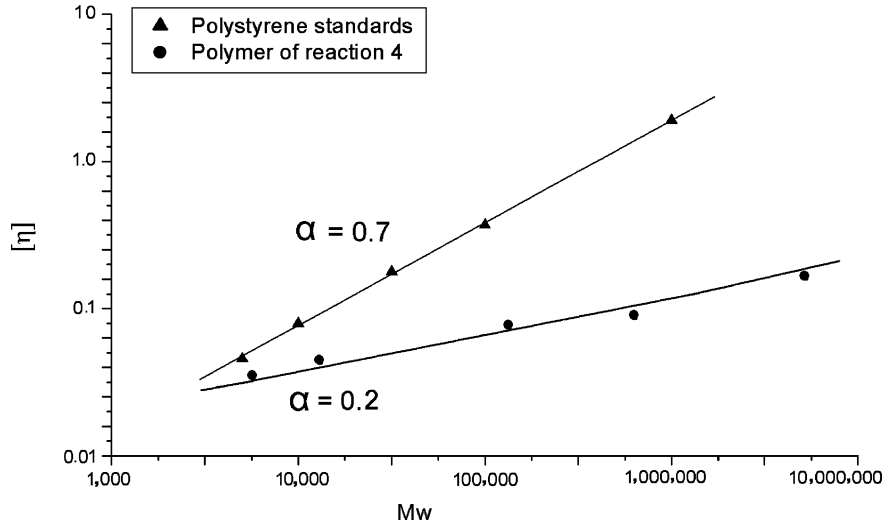

Figure 3. Plot of intrinsic viscosity vs molecular weight for hyperbranched poly(DVB) and linear poly(styrene) standards. The intrinsic viscosities [η] of the hyperbranched poly(DVB) are much lower than those of linear poly(styrene). MHS exponent $\alpha = 0.70$ for poly(styrene) vs 0.20 for the hyperbranched poly(DVB) (entry 4, Table 1).

calculated from [1]H NMR was slightly higher than the molar fraction of initiator incorporated in poly(DVB). Ideally, the molar fraction of the branched DVB should be almost equal to initiator as every branch incorporated into the polymer will bring one branched DVB and one new initiator. This discrepancy may be due to cyclization by intramolecular combination which has already been reported.[26]

$$\frac{\text{branched DVB}}{\text{linear DVB}} = \frac{\left\{[\text{integral of (a + b)}] - \frac{3}{2}[\text{integral of (c + d)}]\right\}/6}{\frac{[\text{integral of (c + d)}]}{2}} \quad (2)$$

Furthermore, the hyperbranched poly(DVB) exhibits interesting solution properties. A classic Mark−Houwink−Sakurada (MHS) plot (Figure 3) shows that the intrinsic viscosity [η] of poly(DVB) is much lower than that of linear polystyrene having an equivalent molecular weight. In addition, the slope of log [η] vs log M_r is much lower (MHS exponent $\alpha = 0.70$ for PSt vs 0.20 for the product of reaction 4 (Table 1), demonstrating a significantly decreased level of interaction between solvent and polymer as is typically encountered in densely branched macromolecules. Finally, the changes of molecular size observed in the DLS data (Figure 4) show solid evidence of hyperbranched poly(DVB). First, the molecular size of poly(DVB) is much smaller than that of the equivalent molecular weight linear polystyrene because of their dense structure. Second, in the complex solution of methanol and THF, poly(DVB) displays much smaller molecular contractions as the addition of the poorer solvating solvent is increased when compared to the effect on linear PS. These data also confirm the hyperbranched nature, as the molecules clearly have much reduced levels of freedom to interact with differing solvents compared to the corresponding linear materials. Clearly, to completely eliminate

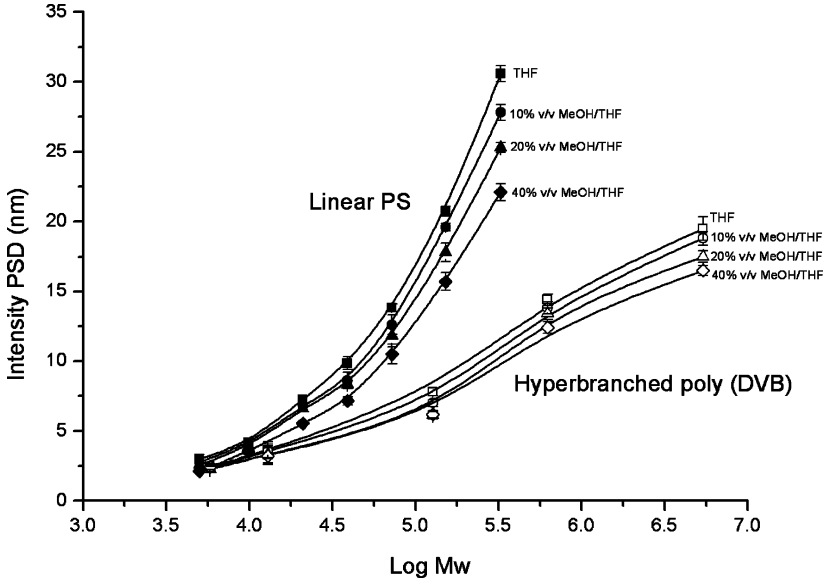

Figure 4. Plot of DLS data showing particle (molecular) size distribution vs log M_w for linear poly(styrene) and hyperbranched poly(DVB) in THF and a series of complex solvent mixtures with methanol. The molecular weights of the polystyrene samples are 5000, 9800, 21000, 39000, 72200, 151700, and 325000 respectively. The poly(DVB) samples are those from entries 1−5 in Table 2.

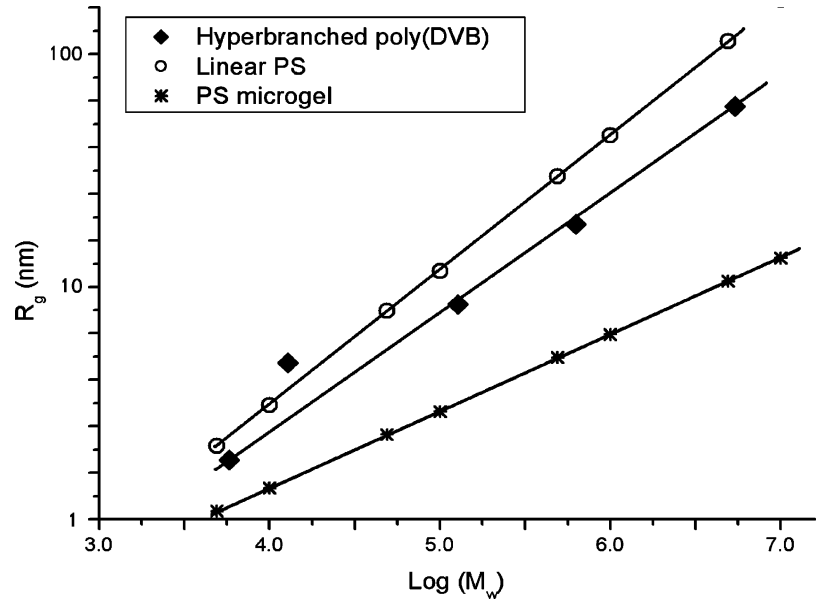

Figure 5. Plot of the radius of gyration vs log M_w. Comparison of the size of hyperbranched poly(DVB) to those obtained from published linear polystyrene and polystyrene microgels.[28] The radius of gyration of hyperbranched poly(DVB) is demonstrated to be quite different from both of linear PS and microgel PS.

the possibility of microgel formation, it would be necessary to specifically synthesize such microgels for comparison. There is only one published example of such a comparison[27] and these authors report that comparisons are not trivial. The root-mean-square (rms) radius $\langle r_g^2\rangle^{1/2}$ (also called the radius of gyration) describes the size of a macromolecular particle in a solution, regardless of its shape or structure. It is important to note that the rms radius is not identical to the geometrical radius for the species. Figure 5 presents the log−log plots of rms vs weight-average molecular weight for linear PS, PS microgel and our hyperbranched poly(DVB) species obtained from GPC−MALLS analysis. The $\langle r_g^2\rangle^{1/2}$ values for the hyperbranched poly-(DVB) samples were obtained directly from the GPC−MALLs data while the corresponding data points presented for the linear polystyrene and microgel examples were obtained from literature data[24,28] and calculation from equations (eq 3)[24] and (eq 4)[28] respectively. It should be noted that the accuracy of the first two poly(DVB) samples is not high because of there is a lower limit to the GPC−MALLS data of approximately 10 nm.

$$\text{linear PS} \quad \langle r_g^2\rangle^{1/2} = 0.014 \times M_w^{0.585} \tag{3}$$

$$\text{PS microgel} \quad \langle r_g^2\rangle^{1/2} = 0.065 \times M_w^{0.333} \tag{4}$$

The results clearly show the radius of gyration from poly-(DVB) is quite different from that of the linear PS and PS microgels. This indicates that the species synthesized in this study are in-fact hyperbranched, because their physical characteristics match neither that of linear or that of microgel materials.

Furthermore, the data demonstrate that the molecular sizes of the branched macromolecules are smaller than those of the linear polymer of a corresponding molecular weight. Thus, as GPC elution volume depends on the molecular size of the polymer, the molecular weight of the branched polymers detected at a particular elution volume should be much higher

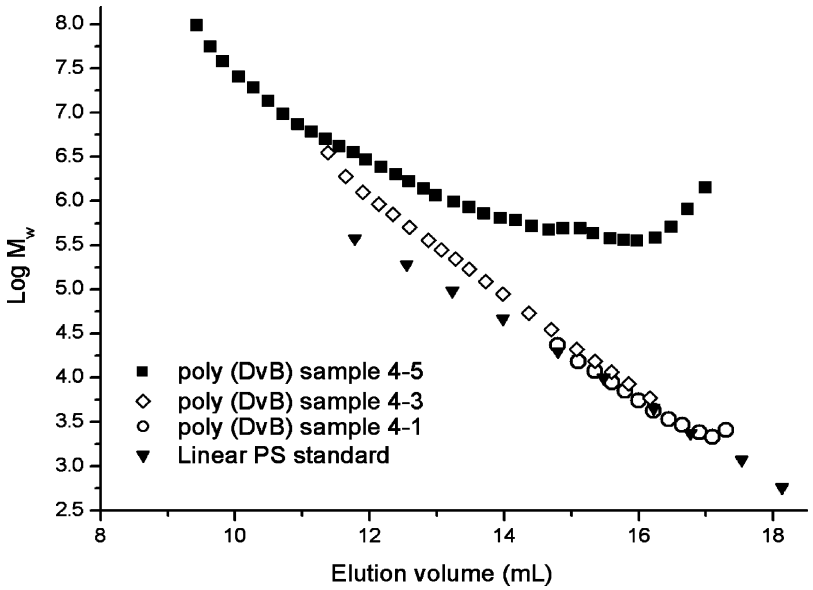

Figure 6. Plot of the log of weight-average molecular weight vs elution volume for the poly(DVB) (entries 1−5, Table 2) and linear PS samples. These data confirm that the poly(DVB) samples are highly branched as they approach high conversion since the plots lie significantly above that of the linear PS.

Table 3. Homopolymerizations of EGDMA by Deactivation Enhanced ATRP[a]

entry	[EGDMA]:[I]:[Cu(I)]:[Cu(II)] (mol ratio)	solvent	temp (°C)	time (h)	$M_n \times 10^{-4}$	PDI	yield (%)
1	50:1:1:0	butanone	60	3			gel
2	50:1:0.5:0	butanone	60	5			gel
3	50:1:0.18:0.03	butanone	65	7	4.4	3.1	38
4	100:1:0.3:0.1	butanone	65	15	4.8	3.5	48
5	50:1:0.188:0.063	THF	60	29	15.0	4.1	63
6[b]	100:1:0:0	THF	60	0.15			gel

[a] For all reactions: [EGDMA] = 1.22 M, [Cu(I)+Cu(II)]/[bpy] = 1:2. Note also that a high ratio of Cu(II)/ Cu(I) significantly slows the reaction rate, leading to high yields of hyperbranched polymer without formation of gels. [b] Azobis(isobutyronitrile) (AIBN) was used as the initiator in reaction 6, a normal radical solution polymerization.

than that of the linear polymer at that volume. Thus, the comparison of the molecular weight against elution volume plots of poly(DVB) and linear PS sample should reveal differences in the behavior of the molecular structures, indicating different levels of branching. Figure 6 demonstrates that the data from poly(DVB) materials are indeed different from those of the linear equivalents thus confirming differences in the structure type and supporting the conclusion that the polymers synthesized are more highly branched because the plots lie significantly above the one for linear PS.[24,25]

Synthesis and Characterization of Hyperbranched Poly-(EGDMA). The mechanism of homopolymerization of hyperbranched poly(EGDMA) is illustrated in Scheme 3 for the ATRP of EGDMA (**1**). First, initiator (**2**) is activated by Cu(I) complex, yielding a new radical chain. Because the Cu(I)/Cu(II) ratio and concentration are chosen specifically for short chain propagation, the new chain only propagates a few times to form a short chain radical (**3**) with many pendent vinyl groups. This short chain radical is subsequently deactivated to form a halogen terminated oligomeric macromonomer (**4**) through halogen transfer catalyzed by Cu(II). This macromonomer (**4**) is reinitiated by the Cu(I) complex leading to the same propagation process and halogen transfer. If macromonomer (**4**) is incorporated into the chain, it forms a branching point (**5**). Every macromonomer incorporated generates a branching point, which gives rise to a highly branched structure (**6**) with many halogen and vinyl end functional groups.

A series of EGDMA polymerizations were conducted under different reaction conditions (Table 3). As the reactivity of methacrylate monomers is generally higher than styrenic monomers with the ATRP system used in this study, we have change two conditions to further slow down the polymerization: first, 2-methyl chloropionate and $CuCl/CuCl_2$ were used instead of bromide initiator and catalyst applied in polymerization of poly(DVB). Second, the monomer concentration is decreased to 1.22 mol/L in this system. Under normal ATRP conditions (entries 1 and 2 in Table 3) gels formed within 3 h due to the rapid polymerization rate. To prevent cross-linking, the reactions were modified to slow the polymerization rate by adding Cu(II). A significant improvement was achieved (entries 3 and 4). To add further control, the total amount of copper catalyst was reduced relative to initiator, i.e., [I]/[Cu(I) + Cu(II)] from 2.5/ 1 to 4/1 (entries 5), the strong polar solvent 2-butanone was replaced by less polar THF and a slightly lower temperature was adopted. Under these conditions, the growth of polymer chains was greatly decreased, cross-linking was suppressed leading to higher yields of soluble hyperbranched polymer. The most significant result (entry 5) is the attainment of a high yield, 63% after 29 h polymerization. Beyond this point, we clearly see that gelation begins to occur, and extending to higher yield is one of our future targets. By contrast, under normal free radical polymerization conditions, a gel is formed almost instantly.[29,30] The results give further solid evidence to demonstrate successful synthesis of poly(DVB).

Monitoring of the polymerization process using GPC equipped with both RI and MALLS detectors clearly demonstrates the influence on the polymerization of the reversible activation (or deactivation) controlled hyperbranched polymerization mechanism (Figure 7, Figure 8, and Table 3). The molecular weight of the polymers increases with monomer conversion, demon-

Scheme 3. Mechanism for Homopolymerization of EGDMA via Deactivation Enhanced ATRP

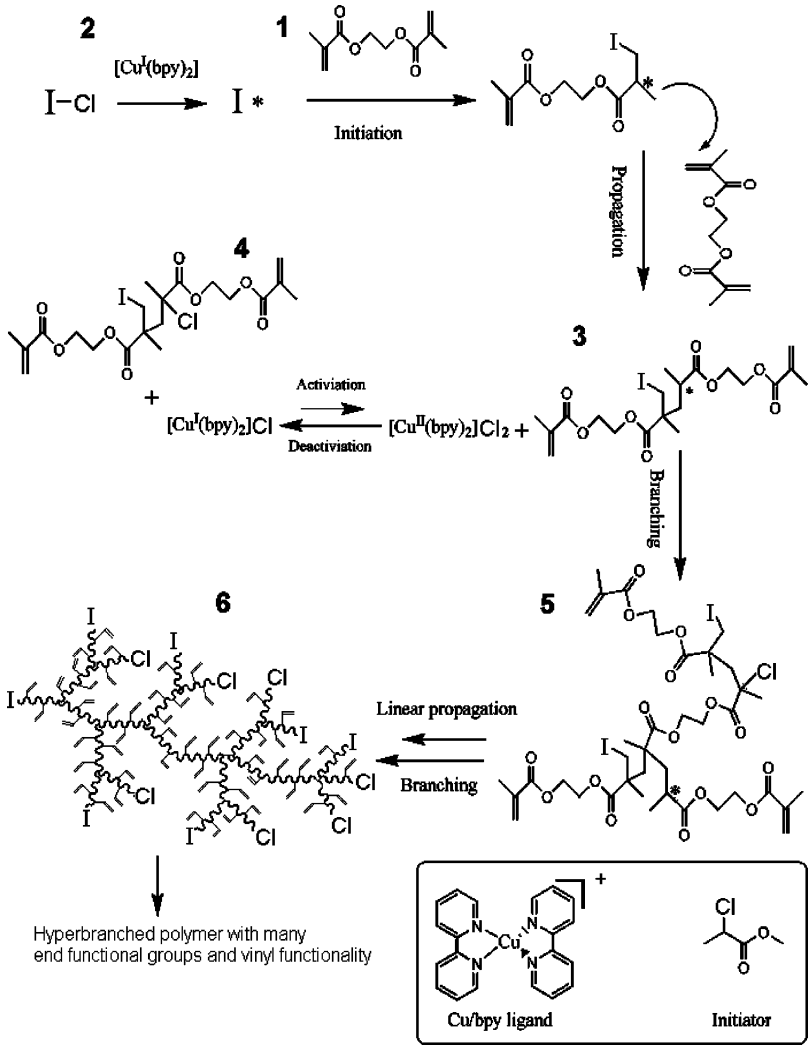

strating a living polymerization process. The molecular weight distribution broadens with increasing monomer conversion, as is commonly observed in synthesis of hyperbranched polymers. However, it is worth noting that in the initial stages of the polymerization process, the molecular weight of the polymer increases with monomer conversion, but they retain narrow polydispersity. This is because at low monomer conversion the propagation mainly leads to linear polymer chains with a low

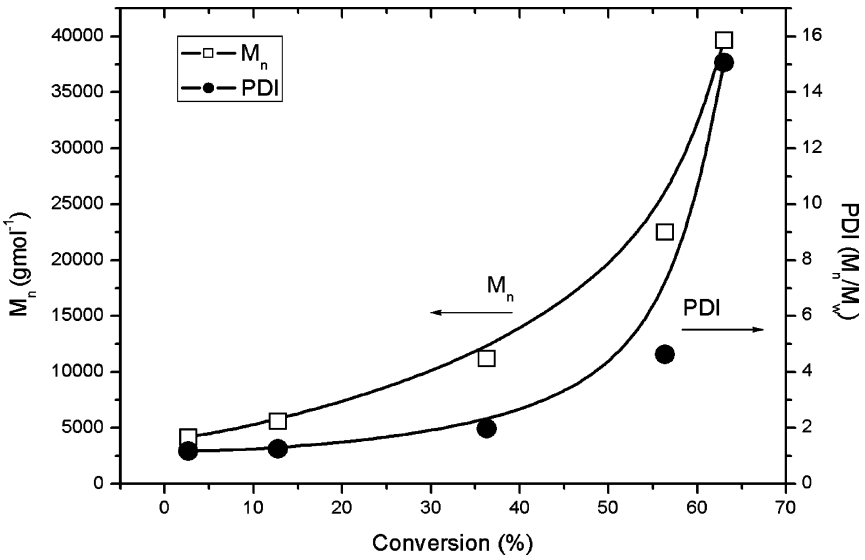

Figure 7. Plot of the weight-average molecular weight and molecular weight distribution of poly(EGDMA) (M_n (□) and PDI (●)) vs monomer conversion for the deactivation enhanced ATRP of EGDMA, Reaction conditions: [EGDMA] = 1.22 M, [EGDMA]:[I]:[Cu(I)]:[Cu(II)] = 50:1:0.188:0.063, [Cu(I) + Cu(II)]/[bpy] = 1:2, T = 60 °C (entry 5 in Table 3).

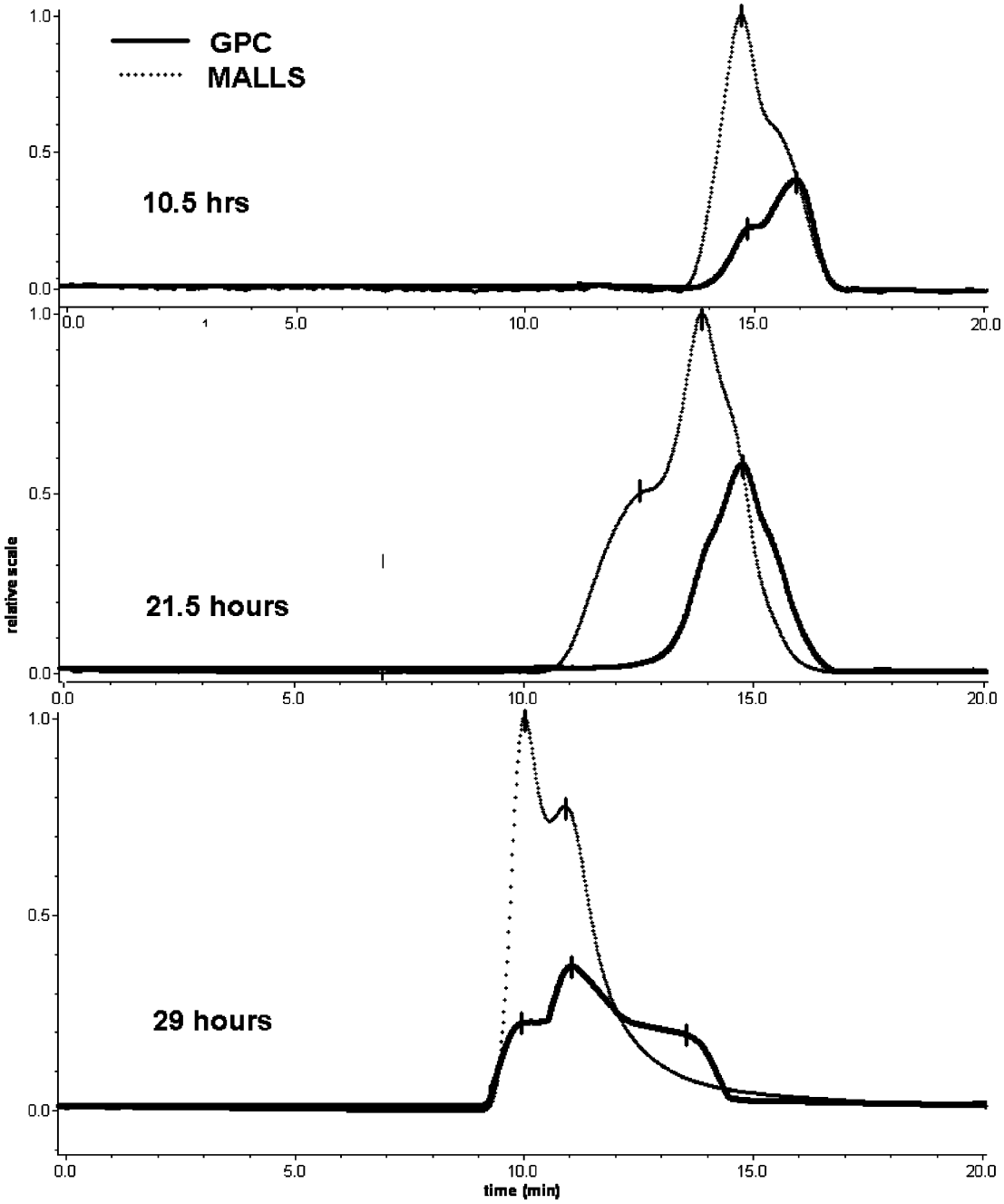

Figure 8. MALLS and RI chromatograms of GPC analysis for poly(EGDMA) samples (entries 5−3 to 5−5 in Table 4). Note, the evolution of molecular weight and molecular weight distribution with reaction time showing the formation of hyperbranched polymer.

Table 4. Hyperbranched Poly(EGDMA) Samples Collected at Different Reaction Times for the Reaction 5 in Table 3[a]

			GPC results			MALLS results			
sample	reaction time (h)	yield (%)	M_n (g mol^{-1})	M_w (g mol^{-1})	PDI	M_n (g mol^{-1})	M_w (g mol^{-1})	PDI	branch ratio[b]
5−1	2.0	3.0	4100	4800	1.16	4370	5106	1.17	0.15
5−2	3.8	13.1	5500	7000	1.25	6915	9710	1.40	0.21
5−3	10.5	36.5	9481	13 908	1.46	12 210	21 890	1.79	0.25
5−4	21.5	55.4	20 434	43 354	1.69	33 530	72 030	2.15	0.31
5−5	29.0	63.0	150 084	607 320	4.05	861 300	3 244 000	3.78	0.45
5−6	30.5	66.0	gelation						

[a] Reaction conditions: [EGDMA] = 1.22 M, [EGDMA]:[I]:[Cu(I)]:[Cu(II)] = 50:1:0.188:0.063, [Cu(I) + Cu(II)]/[bpy] = 1:2, T = 60 °C. [b] Determined by NMR spectrum.

level of branching (see entry 1 in Table 4). As the reaction proceeds with multifunctional monomer, the molecular weight of polymer increases much faster than normally expected for ATRP (see entries 2−5 in Table 4). This is because at later stages of polymerization, significant levels of the monomer and lower molecular weight oligomers have been consumed and the reactions tend toward branching rather than linear growth. Furthermore, the reaction again demonstrated a monomer

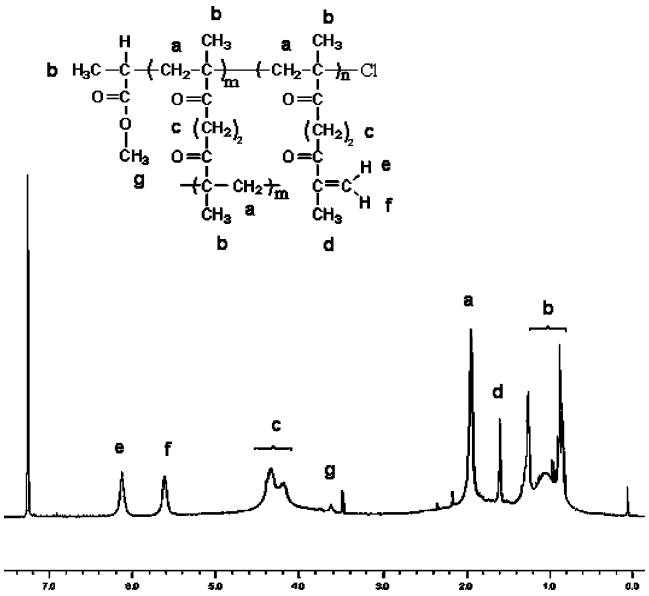

Figure 9. ^{1}H NMR spectrum of poly(EGDMA). The significant concentration of peaks e and f relative to peak c demonstrate a high branch ratio for the poly(EGDMA). Clearly, there is potential for hyperbranched polymers which contain high levels of pendant vinyl groups to cross-link during further polymerization. However, this is not thought to be the case here because the samples are completely soluble in solvent of choice (THF or $CDCl_3$).

conversion ceiling of approximately 60% as in the poly(DVB) case, indicating that at this point the molar fraction, steric bulk and molecular mobility effects that are inhibiting gelation are reduced to a point that gel formation begins to take place. The data show that the measured MALLS molecular weight is always higher than the RI results (Figure 8 and Table 4), which also strongly support formation of a hyperbranched architecture.[24] At this point, it must be stressed that, as with the DVB case, the GPC and MALLS data for sample number 5 have been included (Table 4 and Figure 8) for comparison with the materials sampled at earlier points in the reaction only to demonstrate that the molecular weight of the hyperbranched material is still rising at this point but has not yet become an insoluble gel. Again the MALLS data are predicting that sample 5 has a significant component of its molecular weight distribution above the upper exclusion limit of the system (upper limit is 2 million Da (M_w)) and thus cannot be treated as giving either a definitive molecular weight or polydispersity data.

The hyperbranched structure of poly(EGDMA) was also confirmed by NMR (Figure 9). The chemical shift data are summarized as follows: δ 0.90−1.40 (backbone CH_3, b), 1.91 (terminal CH_3, d), 2.18 (backbone CH_2, a), 4.05−4.43 (CH_2-CH_2, c), 5.60 (terminal C═CH, f), 6.12 (terminal C═CH, e), 7.26 (solvent). From the NMR spectrum, the ratio of branched EGDMA units was calculated by comparison of the integrals of the peaks for the backbone protons (a, b) and vinyl protons (e, f). The ratio between the branched EGDMA to the linear EGDMA is calculated as shown in eq 3:

$$\frac{\text{branched EGDMA}}{\text{linear EGDMA}} = \frac{\left[\frac{(\text{integrals of c})}{4} - (\text{integrals of e})\right]}{\text{integrals of e}} \quad (5)$$

The ratio of branched EGDMA to linear EGDMA was calculated to be *ca.* 0.45:1 (sample 5−5 in Table 4), which agrees with a hyperbranched structure. Branching ratios of this level, while successfully achieving the synthesis of soluble hyperbranched polymers via a one-step free radical polymerization have never been reported before.[20,29] The difference in intrinsic viscosity ([η]) between PEGDMA and linear PMMA further supports the hyperbranched structure within these polymers. A classical Mark−Houwink−Sakurada (MHS) plot (Figure 10) shows that the intrinsic viscosity of poly(EGDMA) is much lower than that of PMMA of similar molecular weight. In addition, the lower slope of log [η] vs log M_w indicates less interaction between solvent and the highly branched polymer.[14,18,31]

Conclusion

Through deactivation enhanced ATRP, novel dendritic poly(DVB) and poly(EGDMA) polymers have been successfully prepared from homopolymerizations of commercially available multifunctional vinyl monomers. No cross-linking or microgel

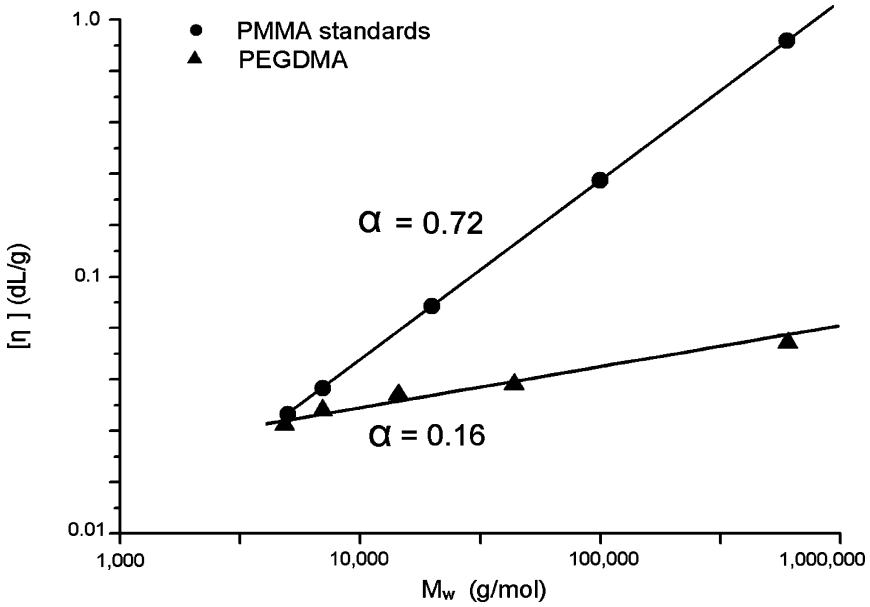

Figure 10. Plot of intrinsic viscosity vs weight-average molecular weight for hyperbranched PEGDMA and linear PMMA. The intrinsic viscosities [η] of the hyperbranched poly(EGDMA) are much lower than those of linear PMMA. MHS exponent $\alpha = 0.72$ for PMMA vs 0.16 for the hyperbranched poly(EGDMA) (entry 5, Table 3).

was observed in the polymer provided that the overall monomer conversion is kept below 60%. This figure being far in excess of the yield that can be obtained with such high levels of branching via any other polymerization mechanism attempted to date. These new dendritic poly(DVB) and poly(EGDMA) polymers possess highly branched structures with a multiplicity of reactive vinyl and halogen end functional groups, and controlled chain structure. We believe that this new strategy for preparation of hyperbranched polymers could open up the field to the polymerization of a very wide range multifunctional vinyl monomers or combinations of comonomers in any proportion. We have demonstrated that this strategy may be applied to ATRP, but could in principle be applied to other vinyl polymerization mechanisms, e.g., radical, cationic, group transfer, or ligated anionic polymerization depending on the nature of the initiation system and of the external stimulus that is applied. We believe that this new approach could have a major impact on the preparation and application of hyperbranched materials.

Acknowledgment. The authors thank the University of Nottingham, Institute of Materials (UNIMAT), EPSRC and Uniqema for their support. SMH holds a Royal Society-Wolfson Research Merit Award. D.J.I. is appointed to the DICE (Driving Innovation in Chemistry and Chemical Engineering) Initiative at the University of Nottingham.

Supporting Information Available: Figure showing the time dependence of monomer conversion during ATRP of DVB. This material is available free of charge via the Internet at http://pubs.acs.org.

References and Notes

(1) Frechet, J. M. J. *Science* **1994**, *263* (5154), 1710−1715.
(2) Tomalia, D. A.; Frechet, J. M. J. *J. Polym. Sci. Part A: Polym. Chem.* **2002**, *40*, 2719−2728.
(3) Tomalia, D. A.; Brothers, H. M.; Piehler, L. T. *Abstr. Pap. Am. Chem. Soc.* **1995**, *210*, 39-PMSE.
(4) Tomalia, D. A.; Baker, H.; Dewald, J.; Hall, M.; Kallos, G.; Martin, S.; Roeck, J.; Ryder, J.; Smith, P. *Polym. J.* **1985**, *17* (1), 117−132.
(5) Cooper, A. I.; Londono, J. D.; Wignall, G.; McClain, J. B.; Samulski, E. T.; Lin, J. S.; Dobrynin, A.; Rubinstein, M.; Burke, A. L. C.; Frechet, J. M. J.; DeSimone, J. M. *Nature* **1997**, *389* (6649), 368−371.
(6) Gillies, E. R.; Frechet, J. M. J. *Drug Discovery Today* **2005**, *10* (1), 35−43.
(7) Tomalia, D. A. *Adv. Mater.* **1994**, *6*, 529−539.
(8) Tomalia, D. A. *Macromol. Symp.* **1996**, *101*, 243−255.
(9) Tomalia, D. A.; Naylor, A. M.; Goddard, W. A. *Angew. Chem., Int. Ed. Engl.* **1990**, *29* (2), 138−175.
(10) Jikei, M.; Kakimoto, M. *Prog. Polym. Sci.* **2001**, *26* (8), 1233−1285.
(11) Kim, Y. H. *J. Polym. Sci. Part a: Polym. Chem.* **1998**, *36*, 1685−1698.
(12) Kim, Y. H.; Webster, O. W. *J. Am. Chem. Soc.* **1990**, *112*, 4592−4593.
(13) Kim, Y. H.; Webster, O. W. *Macromolecules* **1992**, *25*, 5561−5572.
(14) Frechet, J. M. J.; Henmi, M.; Gitsov, I.; Aoshima, S.; Leduc, M. R.; Grubbs, R. B. *Science* **1995**, *269* (5227), 1080−1083.
(15) Hawker, C. J.; Frechet, J. M. J.; Grubbs, R. B.; Dao, J. *J. Am. Chem. Soc.* **1995**, *117*, 10763−10764.
(16) Matyjaszewski, K.; Gaynor, S. G.; Kulfan, A.; Podwika, M. *Macromolecules* **1997**, *30*, 5192−5194.
(17) Costello, P. A.; Martin, I. K.; Slark, A. T.; Sherrington, D. C.; Titterton, A. *Polymer* **2002**, *43*, 245−254.
(18) Guan, Z. *J. Am. Chem. Soc.* **2002**, *124*, 5616−5617.
(19) Sato, T.; Sato, N.; Seno, M.; Hirano, T. *J. Polym. Sci. Part A: Polym. Chem.* **2003**, *41*, 3038−3047.
(20) Isaure, F.; Cormack, P. A. G.; Graham, S.; Sherrington, D. C.; Armes, S. P.; Butun, V. *Chem. Commun.* **2004**, *9*, 1138−1139.
(21) Liu, B. L.; Kazlauciunas, A.; Guthrie, J. T.; Perrier, S. *Macromolecules* **2005**, *38*, 2131−2136.
(22) Matyjaszewski, K.; Patten, T. E.; Xia, J. H. *J. Am. Chem. Soc.* **1997**, *119*, 674−680.
(23) Patten, T. E.; Xia, J. H.; Abernathy, T.; Matyjaszewski, K. *Science* **1996**, *272* (5263), 866−868.
(24) Podzimek, S. *J. Appl. Polym. Sci.* **1994**, *54* (1), 91−103.
(25) Baudry, R.; Sherrington, D. C. *Macromolecules* **2006**, *39*, 1455−1460.
(26) Li, Y. T.; Armes, S. P. *Macromolecules* **2005**, *38*, 5002−5009.
(27) Kharchenko, S. B.; Kannan, R. M.; Cernohous, J. J.; Venkataramani, S. *Macromolecules* **2003**, *36*, 399−406.
(28) McGrath, K. J.; Roland, C. M.; Antonietti, M. *Macromolecules* **2000**, *33*, 8354−8360.
(29) Wang, W. X.; Yan, D. Y.; Bratton, D.; Howdle, S. M.; Wang, Q.; Lecomte, P. *Adv. Mater.* **2003**, *15*, 1348.
(30) Jiang, C. F.; Shen, Y. Q.; Zhu, S. P.; Hunkeler, D. *J. Polym. Sci., Part A: Polym. Chem.* **2001**, *39*, 3780−3788.
(31) Mourey, T. H.; Turner, S. R.; Rubinstein, M.; Frechet, J. M. J.; Hawker, C. J.; Wooley, K. L. *Macromolecules* **1992**, *25*, 2401−2406.

MA0707133